A polarizable continuum approach for the study of heterogeneous dielectric environments

ARTICLE *in* THE JOURNAL OF CHEMICAL PHYSICS · JUNE 2006

Impact Factor: 2.95 · DOI: 10.1063/1.2188392 · Source: PubMed

5 AUTHORS, INCLUDING:

Maria francesca Iozzi
University of Oslo
21 PUBLICATIONS **408** CITATIONS
SEE PROFILE

Maurizio Cossi
Amedeo Avogadro University of Eastern Pied…
98 PUBLICATIONS **19,490** CITATIONS
SEE PROFILE

Roberto Improta
Italian National Research Council
148 PUBLICATIONS **4,664** CITATIONS
SEE PROFILE

Vincenzo Barone
Scuola Normale Superiore di Pisa
772 PUBLICATIONS **43,620** CITATIONS
SEE PROFILE

A polarizable continuum approach for the study of heterogeneous dielectric environments

Maria Francesca Iozzi, Maurizio Cossi, Roberto Improta,
Nadia Rega, and Vincenzo Barone[a)]
Dipartimento di Chimica, Università Federico II, Complesso Monte S. Angelo, via Cintia, I-80126 Napoli, Italy

(Received 12 October 2005; accepted 27 February 2006; published online 11 May 2006)

We present a computational method, exploiting some features of the polarizable continuum model (PCM) to describe heterogeneous media; it belongs to the family of electrostatic embedding mixed methods, such as the more common quantum-mechanical (QM)/molecular mechanics approaches, with the electrostatic long range effects accounted for by a polarized continuum instead of atomic point charges. Provided effective dielectric constants are determined for the various parts of the system, the method is much faster than its atomistic counterpart, and allows for high-level QM calculations on the fragment of interest, using all the highly efficient computational tools developed for homogeneous PCM. Two case studies (the calculation of the pK_a of solvent exposed acidic residues in a model protein, and the calculation of the electron spin resonance spectrum of a typical spin probe partially embedded in a membrane) are analyzed in some detail, to illustrate the application of the method to complex systems. © *2006 American Institute of Physics*. [DOI: 10.1063/1.2188392]

I. INTRODUCTION

The computational study of large/complex systems, such as biomolecules or nano-surfaces, still represents a challenging task, due to the high computational costs and the difficulties to accurately treat the subtle balance of different physicochemical effects (electronic/steric, statical/dynamic, intrinsic/environmental) modulating their behavior. One of the most fruitful strategies to study those kinds of systems consists in defining a suitable subsystem, the most relevant for the property or the process under investigation (the core). This part is treated at the highest level of accuracy, whereas the effect of the remaining part of the system, considered as a perturbation, is taken into account at a more approximate level.

Within this general framework, the different procedures are characterized by (i) the number of subsystems in which the whole system is partitioned, (ii) the level at which each part is treated, and (iii) the way in which the interaction among the different parts is accounted for. Of course, the nature of the system or of the process under study suggests the most suitable approach. In this respect, a reliable description of several important processes and properties requires that at least the inner part of the system is treated by accurate quantum-mechanical (QM) methods. Examples of such situations involve spectroscopic parameters,[1–4] electron transfer processes, photochemical reactions,[5,6] etc. Mixed QM-molecular mechanics (MM) methods can be considered paradigmatic approaches to treat those systems: here the external part is treated at the MM level, while its effect on the core can be usually accounted for by simple electrostatic interactions. Although this approach has been successfully applied to the study of many important processes,[7,8] its "atomistic" nature requires a detailed knowledge of the structure of the whole system and, when using electrostatic embedding, the selection of suitable atomic charges (and, possibly, polarizabilities) to describe the interactions between QM and MM regions. The computational cost of QM/MM approaches increases significantly when the effect of a liquid environment has to be included too: for instance, many properties of water-soluble proteins[9–11] depend on the interaction of some residues both with the solution and with the bulk protein. Treating such a case by embedding the whole QM/MM system in a continuum solvent would require very large cavities and a correspondingly large number of solvation charges. Another example is the study of small-molecule permeants embedded in a lypid bilayer, which can be correctly modeled only by introducing both the solvent and the bilayer effects. In this case, the atomistic description can be even more complex, as the penetration of the probe induces a distorsion of the lypid layer that is not easy to reproduce without lenghty molecular dynamics.

However, a full atomistic approach is not always strictly necessary.[12–15] Previous studies[9] suggest that pK_a the of a residue in prion protein is influenced by the direct interaction between the residue itself and few neighboring groups, while the presence of the remaining protein body can be described quite accurately in terms of its average effect. Accordingly, detailed structural information can be avoided in favor of a continuum description of the protein body through an *ad hoc* protein bulk dielectric constant.[16]

Recently, this approach (treating part of the system outside a given region of interest as a dielectric continuum) has become very popular. Within the generalized Born formal-

[a)]Author to whom correspondence should be addressed. Fax: +39 081 674090. Electronic mail: baronev@unina.it

ism, Stern and Feller have resolved the electrostatics of parts inside a lipid bilayer,[12] while the same formalism was adopted by Tanizaki, Im, and co-workers for modeling biologic membranes.[13,14]

On the other hand, the so-called polarizable continuum model[17] (PCM) has been widely extended and generalized, in order to provide an accurate and effective description of complex systems such as polypeptides and proteins, offering an attractive alternative for the study of environmental effects in macromolecular systems.[9,17–21] PCM is the most used continuum solvation model for accurate quantum-mechanical applications, and it has been applied to a wide range of problems, from structure, to thermodynamics, kinetics, and spectroscopy in both isotropic and anisotropic environments.[21–23] Further developments now allow the study of solvation effects on molecules at the interface between two fluid phases, i.e., in situations where the electric permittivity depends on the position.[24–26]

Actually, there are several processes that can be modeled as occurring at the interface between two media of different dielectric constant. Typical examples are all those systems in which the region of interest is partly solvent exposed and partly embedded in a macrostructure, i.e., systems experiencing heterogeneous environments. Many processes occurring on the solvent-exposed surfaces of proteins, liquid bilayers, micelles, can thus be profitably studied in this theoretical framework.

In this paper we further explore the use of continuum models to study such *generalized interfaces*, extending the range of application of PCM to treat environmental effects in processes involving macromolecular systems, especially those involving two or more media with different polarity. The proposed model will be validated on two different systems, involving the computation of spectroscopic and energetic properties in heterogeneous media:

(1) The computation of the pK_a of a solvent exposed histidine residue (namely, His140) in prion protein (Fig. 1);
(2) The evaluation of the nitrogen isotropic hyperfine splitting (hfs) of a spin-probe piperidine nitroxyl radical (hereafter tempo, see Fig. 2) interaction with a biological membrane.

Besides their illustrative purposes, both systems have an intrinsic interest. The importance of proton transfer reactions in several processes of biological relevance and the difficulties in determining experimentally the pK_a's within proteins give account for the widespread interest for reliable and effective computational approaches to evaluation.[27] We choose to study the pK_a of a histidine residue (His140) of the human prion protein (hereafter $HuPr^P$), since the transition from the normal cellular prion protein (PrP^C) to a misfolded isoform (PrP^{Sc}) has been recognized as the most significant pathogenic event[28,29] in several neurodegenerative diseases. Furthermore, recent experimental[30–32] and computational[33–35] studies suggest that the conformational rearrangements induced by low *p*H conditions bear significant similarity with

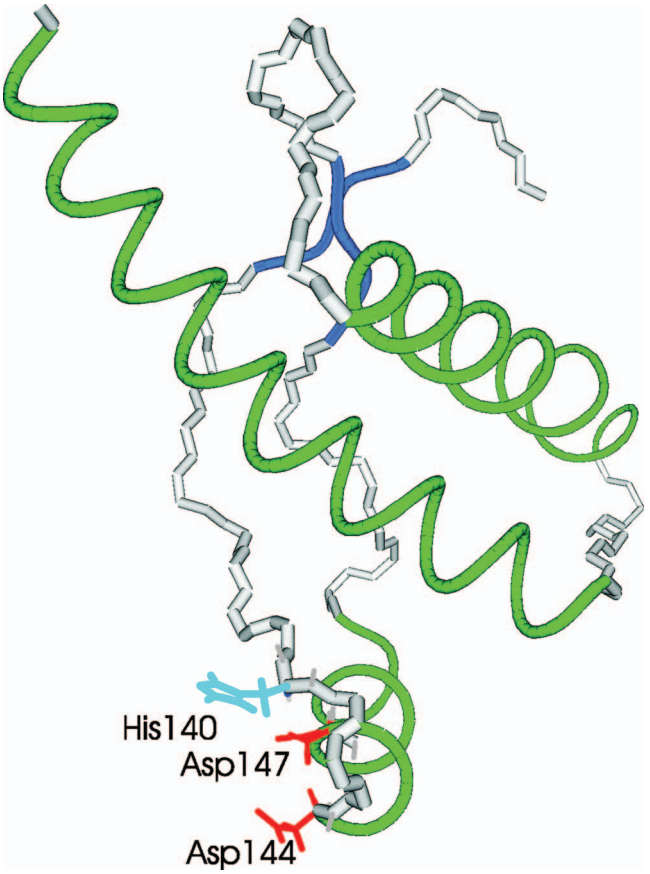

FIG. 1. (Color) Sketch of human prion protein (125–228). The highlighted residues are treated at the QM level.

the transition leading to the misfolded isoform, and that the protonation of one of the four histidine residues present in the *C*-terminal region of $HuPr^P$, the structured core (125-228 aa) of the protein, should play a significant role in this transition.

From another point of view, "spin probing" and "spin labeling" techniques[36,37] have emerged in the last decades as two powerful methods for the study of complex systems (e.g., proteins, micelles, vescicles) by means of electron spin resonance (ESR) spectroscopy. Their use relies on the fact that the magnetic properties of free radicals are modulated by the macroscopic and microscopic features of their environment: polarity, hydrogen bonding power, *p*H, and viscosity of the embedding medium, proximity with other free radicals or charged species, and so on.[38–40] Nitroxide radicals are especially well suited to this end, since they couple a remarkable chemical stability with a localized spin density whose partitioning between N and O atoms is particularly sensitive to electrostatic effects.

II. COMPUTATIONAL METHOD

Isotropic solutions can be accurately described by the PCM:[17,41] the most recent PCM version, designed to take into proper account also the so-called outlying charge effects (due to the solute electronic density tails, that penetrate into the solvent)[42–44] is presented, e.g., in Ref. 45. A quite popular variant of the method is the conductorlike screening

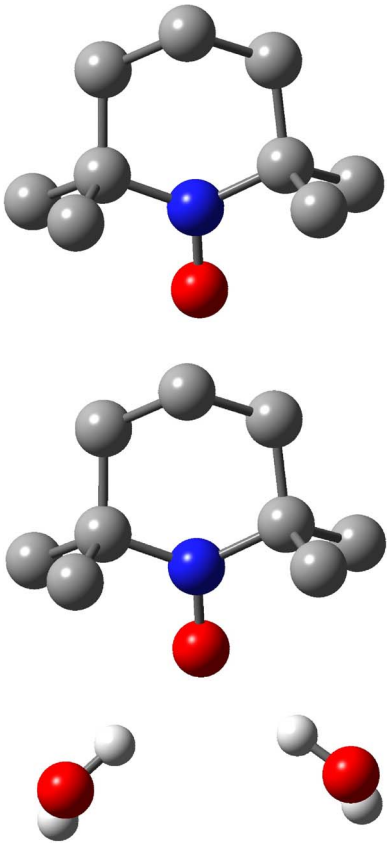

FIG. 2. Piperidine nitroxyl radical (Tempo): isolated (top) and hydrogen-bounded (bottom) to two water molecules. Both structures were optimized at PBE0/6-31g(d) level.

model[46,47] (corresponding to the PCM limit for infinite dielectric constant, but used with satisfactory results also for solvent of rather low polarity): its implementation in the PCM framework (referred to as conductor-PCM, CPCM) is described in Ref. 48.

In all the PCM variants the solute or the region of interest is represented in atomic details and embedded in a cavity formed by the envelope of spheres centered on the solute atoms. The united-atom topological model[49] (UA0) can be used to assign the atomic radii; the procedures to form the cavity are described in detail elsewhere.[50,51] Here we only recall that the cavity surface is finely subdivided in small tiles (*tesserae*), and that the solvent reaction field is described in terms of apparent point charges appearing in tesserae and self-consistently adjusted with the solute electron density (ρ).[45]

The solute-solvent interaction energy is

$$E_{\mathrm{int}} = \mathbf{V}^{\dagger}\mathbf{q} = \sum_{i}^{\mathrm{tesserae}} V_i q_i, \tag{1}$$

where the column vectors $\mathbf{V}$ and $\mathbf{q}$ collect the solute (nuclear+electronic) electrostatic potential and the solvation charges in the surface tesserae, respectively. If $E^0 = E[\rho^0] + V_{\mathrm{NN}}$ is the solute energy *in vacuo*, the quantity that is variationally minimized in the presence of the solvent is the free energy,[45]

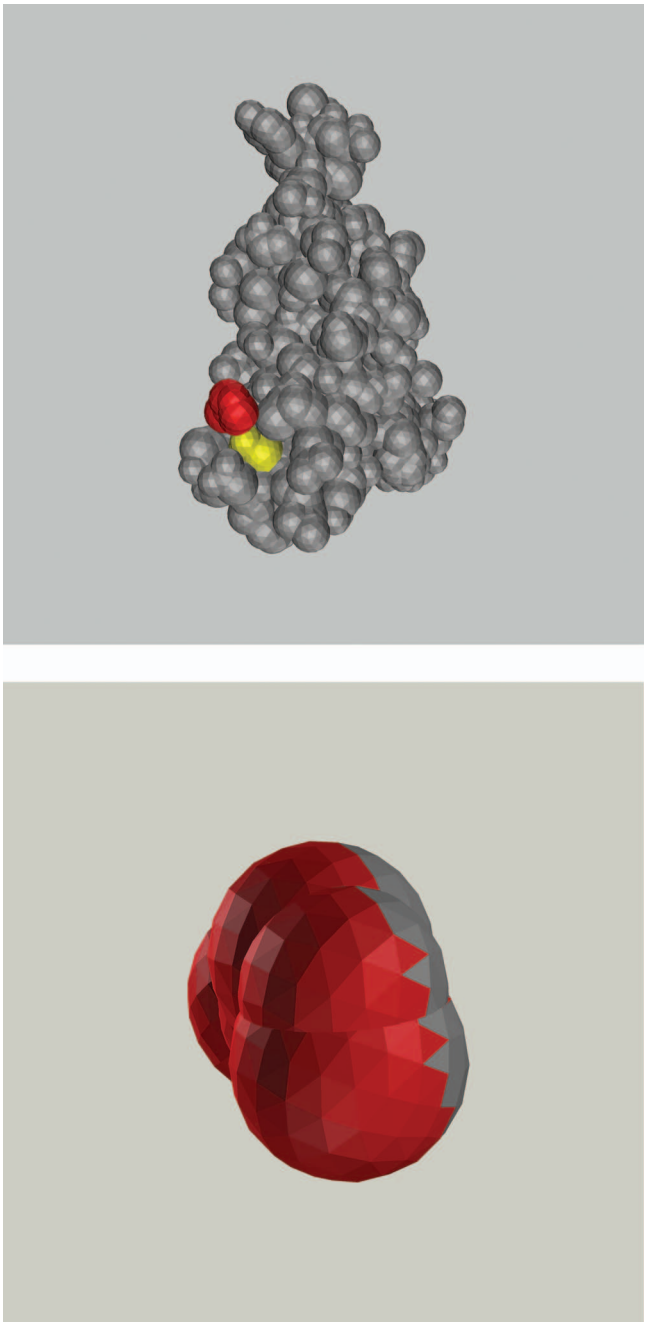

FIG. 3. (Color) The mixed-ϵ cavity (at bottom, for model I) is shaped as the cavity of the *isolated* part of interest. Once the number of different local environments has been defined, the dissection of the cavity surface into two (or more) subregions is made by analyzing the position of each tesserae in the framework of the whole environment. In more details, each tesserae will be "exposed" to one local environment if it is enough close to at least one neighboring group of such an environment, the limiting distance being the solvatation radius of the group itself.

$$G = E[\rho] + V_{\mathrm{NN}} + \tfrac{1}{2}E_{\mathrm{int}} = E[\rho] + V_{\mathrm{NN}} + \tfrac{1}{2}\mathbf{V}^{\dagger}\mathbf{q}, \tag{2}$$

where V_{NN} is the solute nuclear repulsion energy, ρ^0 is the solute electron density for the isolated molecule, and ρ is the corresponding density perturbed by the solvent.

The solvation charges are computed as $\mathbf{q}=\mathbf{QV}$, where $\mathbf{Q}$ is a geometric matrix, depending on the position and size of the surface tesserae. The PCM operator, defined by differentiating the quantity $\frac{1}{2}\mathbf{V}^{\dagger}\mathbf{QV}$ with respect to the electronic

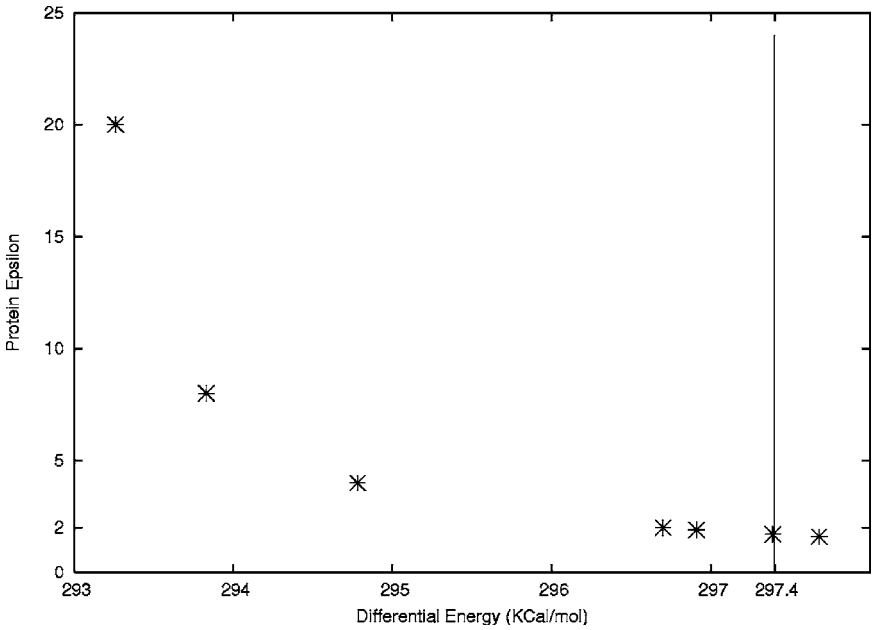

FIG. 4. Differential energies (in kcal/mol) for model II, evaluated with PCM mixed-ϵ model, at different protein dielectric constant. Values are compared with the differential energies of the model system embedded by the protein atomic charges (see Table II).

density is used to correct the Fock or Kohn-Sham operator in the self-consistent field (SCF) procedure, as well as in the calculation of electronic properties. It is worth noting that since the solvation charges depend on the solute potential, and hence on its electronic density, the PCM term in the Hamiltonian is analogous to the Coulomb operator (i.e., a two-electron term, bilinear in the electronic density, that can be put in a pseudo-one-electron form during the SCF procedure).

The core of the model is the definition of the **Q** matrix. For isotropic solvents it is defined as[45]

$$\mathbf{Q} = \mathbf{T}^{-1}\mathbf{R},$$

$$\mathbf{T} = \frac{\epsilon + 1}{\epsilon - 1}\mathbf{S} - \frac{1}{2\pi}\mathbf{DAS}, \tag{3}$$

$$\mathbf{R} = -\mathbf{I} + \frac{1}{2\pi}\mathbf{DA}, \tag{4}$$

where ϵ is the dielectric constant, **I** is the unit matrix, **A** is a diagonal matrix collecting the area of tesserae, and the matrices **S** and **D** are related to the electrostatic potential and to the electric field generated by the solvation charges, respectively.

The treatment can be extended to heterogeneous environments by means of a position-dependent dielectric permittivity, i.e., substituting the dielectric constant by a function $\epsilon(\mathbf{r})$.[25,26] Such an approach requires the knowledge of the electrostatic Green function associated to the particular environment under study: in general this function is not easily defined for nonhomogeneous systems, and must be computed numerically with suitable molecular dynamics. The complexity of the Green function procedure practically prevents its extensive application to large systems such as proteins and membranes: the present approach, on the contrary, is based on the parametric definition of the dielectric function in the different phases, leading to a simple extension of the homogeneous PCM formalism.

To do that, the above equations can be conveniently adapted by replacing the dielectric constant ϵ with a function $f_\epsilon(\mathbf{s})$ defined at any point **s** of the cavity surface. In the computational practice a vector $\mathbf{f}_\epsilon$ is defined on surface tesserae, and Eq. (3) is modified accordingly,

$$\mathbf{T} = \frac{\mathbf{f}_\epsilon + 1}{\mathbf{f}_\epsilon - 1}\mathbf{S} - \frac{1}{2\pi}\mathbf{DAS}.$$

Since **S** and **D** matrices do not explicitly depend on the dielectric permittivity, the changes with respect to the usual, isotropic PCM are quite limited, and the same computational strategy and algorithms for the resolution of the electrostatic problem can be used. It is worth noting that this approach is not intended to describe real liquid interfaces, because in this case a more complex solvation charge pattern would be required: rather, it belongs to the family of electrostatic embedded QM/continuum mixed methods.

The $\mathbf{f}_\epsilon$ vector contains the local ϵ values to be assigned to each tessera: it depends on the dielectric environment shape and on the position of the solute with respect to the discontinuities. In other words, it is possible to define *subregions* on the cavity surface corresponding to portions of the system exposed to different dielectric media.

In the calculation of histidine pK_a in the prion protein, the fragment of interest was isolated from the protein structure, saturating the valencies with hydrogen atoms: the PCM cavity was built around the isolated residue, and another cavity was defined around the remaining protein backbone. The subregion in contact with the protein environment was identified by intersecting these cavities: in other words, each tessera on the histidine surface was considered embedded in the protein if its center lied inside the backbone cavity, otherwise it was solvated by water. Note that it was not necessary to compute all the tesserae on the protein surface (a step that can be computationally demanding for really large solutes), since only the protein atomic spheres are necessary to define this subregion. The choice of the $\epsilon_{\text{protein}}$ to be assigned

TABLE I. Energy difference (between the protonated and neutral forms) and pK_a of 4-methylimidazole (δ isomer). Reported values are in kcal/mole. Geometry optimizations were performed in vacuum at PBE0/6-31G(d,p) level. Values calculated with a cavity formed by six interlocked spheres centered on each moiety, without extra added spheres.

	ΔE	pK_a
Gas phase	238.92	
Zero point energy	−8.84	
CPCM	290.78(290.90)	8.68
PCM	290.77(290.90)	8.67
Expt.		7.53

TABLE II. Differential energies (kcal/mol) in aqueous solution for the protonated and neutral form of the model systems. Energies in solution were calculated with CPCM. A displacement of atomic charges were included to account for the protein backbone structure. Energies refers to the model compounds alone (0 charge), with all prion atomic charges (all) and eventually with all the charges but the one associated with Asp147 (all-Asp147).

	ΔE		
Charges	Model I	Model II	Model III
0	287.22	295.02	295.60
all	296.42	297.40	297.61
(all-Asp147)	289.98	···	···

to the first subregion is a delicate issue in the modeling of such a system, and will be discussed in detail later.

In the calculation of hfs of tempo interacting with a lypid bilayer, a standard PCM cavity was used to house the spin probe. The membrane was modeled as a multiple layer of infinite dielectric continua so that the dielectric constant ϵ only varies along the direction perpendicular to the membrane surface (namely, the z direction). In particular, we have adopted a three-dielectric model[52] (vide infra), designed on the basis of the dielectric profile of a dipalmitoylphosphatidylcholine (DPPC) lipid bilayer in water resulting from the molecular-dynamics simulation performed by Stern and Feller (see Ref. 53). In more detail, the dielectric constant was set to $\epsilon=2$ in the hydrocarbon region (i.e., $z>0$ Å), to $\epsilon=7$ across the ester-groups region ($-5<z<0$ Å), and to $\epsilon=80$ in the bulk-water region ($z<-5$ Å). As the tempo radical approaches the membrane surface, with the N···O bond along the z axis, the portion of water-embedded surface progressively decreases, in favor of the formation of differently embedded subregions. The subregions results from the intesection between the tempo PCM cavity and the three-dielectric model described above.

Finally, although the procedure was coded in a locally modified version of GAUSSIAN 03,[54] it can be easily implemented in any other package containing the PCM algorithms.

All computations have been performed using the PBE0 hybrid functional[55] and the 6-31G(d,p) basis set except evaluations of isotropic hyperfine couplings for which we used the purposely tailored EPR-II basis set. This computational protocol has been validated in a number of previous studies.[40,56]

III. RESULTS

A. Protonation energies of histidine residue in prion protein

The pK_a has been calculated by the well-known relation

$$pK_a = \Delta G_{aq,AH}/2.303RT, \tag{5}$$

$\Delta G_{aq,AH}$ being obtained according to the procedure described in detail in Ref. 9.

As a first step of our computational analysis we computed the pK_a of methylimidazole in aqueous solution, comparing the results obtained by using different PCM versions (see Table I) and verifying the effect of the spheres added to smooth the cavity surface. The computed pK_a's are in good agreement with experiment, with a discrepancy of less than 1.5 pK unit with respect to the experimental pK_a, i.e., an error ≈2 kcal/mol in the differential free energy in solution. In general terms, the adopted computational model is adequate for the study of large proteins by mixed methods, i.e., wherever general trends are sought rather than quantitative accuracy.

The His pK_a has been calculated by single point PCM calculations on three different model systems I, II, and III differing in the size of the part treated at the quantum-mechanical level (see Fig. 1). In I only the side chain of His140 is treated at the QM level. In II the model system is constituted by the side chain of His140 and Asp147. These two residues are indeed hydrogen bonded in the experimental structure of $HuPr^P$, and the pK_a of His140 is expected to be significantly influenced by the possible formation of a strong salt bridge with Asp147 in pK range in which the Asp side chain is not protonated (i.e., for $pp \geqslant 4$). Finally, in III the model system contains together with His140 and Asp147, also Asp144, i.e., the acid base residue closest to the His140/Asp147 pair (see Fig. 3).

For all of the above models we have compared the results provided by two approaches, differing in the way the effect the residues not included in the QM model has been taken into account, i.e., (i) by the embedding technique or (ii) by using two different dielectric constants (as explained in Section II). Please note that also in the former approach the calculations have been perfomed in aqueous solution, the cavity used in the PCM calulation always containing the whole protein.

Inspection of Table II confirms that the most important inter-residue interaction of His140 is the salt bridge with Asp147. As a matter of fact, when the partial charges of all the residues except Asp147 are included in the calculations the computed protonation free energy is very similar to that obtained on model I alone. Analogously, inclusion of all the charges changes the protonation free energy by more the 10 kcal/mol in model I and by only 2.4 kcal/mol in model II. However, it is noteworthy that 2.4 kcal/mol correspond to a pK_a shift of ≈1.8 units, and thus the cumulative effect of the protein residues is not negligible.

On the other hand, the overall effect of the protein residues cannot be compared with that of a polar solution. As a matter of fact, the protonation energy in aqueous solution of

TABLE III. Energy difference (in kcal/mol) between the protonated and neutral forms of the two different model systems for histidine residue within prion protein. Geometry optimization were performed in vacuum at ONIOM:PBE0/AMBER level. Energies in solution were calculated at PBE0 level.

	ΔE			
	Model I		Model II	
	AH	*A*	AH	*A*
Q	+1	0	0	−1
CPCM	290.23		292.82	
PCM[a]	290.58		292.97	

[a]A simplified cavity (made by six interlocked spheres) was used for the PCM calculation to allow a direct comparison with mixed-ϵ PCM values (see Table I).

the adduct formed by the side chain of Asp147 and His140 (with the geometry they have in prion protein) is much larger than that predicted by the embedding technique (see Table III). This result is not surprising, since only a part of model II is exposed to the solvent within the protein, and the "effective polarity" of the protein is much smaller than that of water (Fig. 4).

Convergence between the two computational approaches used is obtained when an effective dielectric constant of ≈ 2 is assigned to the part of the cavity buried within the protein.

Finally, it is important to highlight that our computational procedure suggests that His140 is protonated at neutral *p*H, since the protonation free energy is larger than in methylimidazole. This indication is in agreement with those provided by other computational studies[35] and by the comparison of the NMR protein structure at different *p*H.[57]

B. Tempo radical in biological membranes

The second case examined is the nitrogen hfs of tempo approching a water embedded membrane surface.

Table IV reports the nitrogen hfs computed for the tempo radical in the gas phase and in aqueous solution. It is well known that the nitrogen hfs in nitroxides increases with the polarity of the embedding medium,[40] and our computations confirm this trend, the value in aqueous solution being larger by about 6% than its counterpart in the gas phase. Of course, a structureless continuum takes into account only long-range electrostatic nonspecific interactions, whereas a proper treatment of hydrogen bonding solvents requires also explicit consideration of specific interactions in the cybotactic region. Following previous studies[40] we have then used a mixed discrete/continuum approach in which a cluster formed by tempo and two water molecules (hydrogen bonded to the nitroxide oxygen atom) are embedded in the polarizable continuum. The increment due to the localized interactions (hydrogen bonds) ($\Delta = 1.7$) is larger than its counterpart related to the electrostatic effect of the polaried medium ($\Delta = 0.8$) and the two effects are nearly additive. It is noteworthy that the overall solvent shift predicted by the composite discrete/continuum model (2.0) is in agreement with the experimental values for a number of representative nitroxides.[40]

TABLE IV. The nitrogen hfs (gauss) of isolated and hydrogen-bond clustered tempo, in air and in water.

Tempo	Isolated	Clustered	$\Delta_{\text{Water-Gas}}$
Gas phase	11.050	12.748	1.7
Water	11.854	13.099	1.2

The nitrogen hfs of isolated tempo was then calculated and reported in Figs. 5 and 6 as a function of its position at the water/membrane interface, checking also for the effect of the orientation of the nitroxide moiety with respect to the membrane surface.

When the nitroxide approaches the surface with the N···O bond along the *z* axis (see Sec. II), namely, with the NO moiety 'perpendicular' to the interface (see Fig. 5), as soon as part of the NO moiety leaves the highly polarized environment (i.e., the water medium in our model) the nitrogen hfs remarkably decreases. Interestingly the nitrogen hfs already reaches almost the lower limiting plateau, corresponding to the spin probe fully embedded in the membrane interior, when the 65% of the molecule is membrane embedded, the remaining part of the tempo still being "water exposed." In our picture this correspond to the tempo radical positioned "across" the membrane, with the NO moiety already entered in the membrane, but with the piperidine tail still experiencing an aqueous environment.

Values of Fig. 5 are also reported in Fig. 6 as a function of the water embedded surface portion (solid line), and compared with the nitrogen hfs values of tempo obtained by considering a "parallel" approach of the NO moiety to the membrane surface (points). A decrement of water-embedded surface leads to a lowering of nitrogen hfs, which is steeper for a "perpendicular" than for a parallel approach. This is not surprising since for similar percentages of water-embedded surface, the NO moiety is less water exposed in the first case. According to this qualitative picture, the parallel approach could be favored over the perpendicular one when the nitroxide bears polar para-and/or metasubstituents.

The curves built taking into account bulk solvent effects have a sigmoidal character (quite step for the perpendicular approach and smoother for the parallel one), suggesting that partially embedded nitroxides exhibit nitrogen hfs intermediate between those found in the water phase and in the inner membrane environment, respectively. This finding can be useful when interpreting the results of spin probing experiments, especially when the role played by explicit solute solvent interactions can be neglected (as is usually the case in non-H-bonding solvents).

When hydrogen bonds with specific water molecules are taken explicitly into account, the computed curve becomes significantly flatter (not reported results), suggesting that it would be not easy to determine the position of the spin probe across the water embedded membrane from its experimental hfs value.

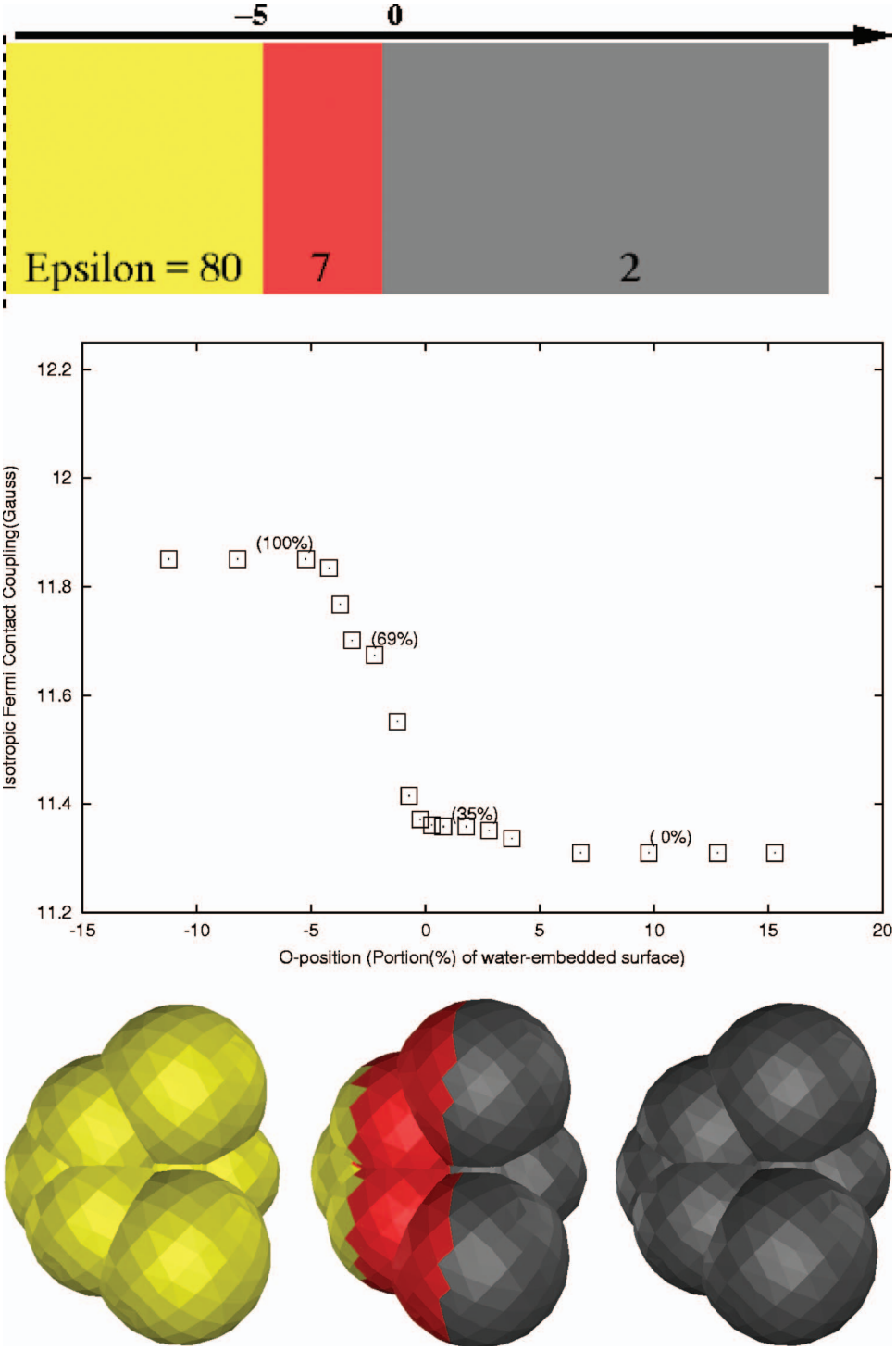

FIG. 5. (Color) The isotropic Fermi contact coupling (gauss) of Tempo across the membrane. Values refers to the isolated tempo molecule entering the membrane via the oxygen atom, with the N–O bond along the z direction. Significant points are highlighted together with the portion of water-embedded surface. All the values were calculated at PBE0/EPR-II level. The cluster geometry was optimized in vacuum at PBE0/6-31g(d). The three dielectric model used to describe the lypid bilayer in water (see text for more details) is shown in the topmost onset.

Obviously the above results must be considered with some caution, since the "experimental" hfs of a spin probe across the membrane is given by the "dynamical" average of different positions with different degrees of embedding. At the same time, as mentioned above, the final estimate of the solvent shift (2 G) is in agreement with previous experimental and computational results.[40]

IV. CONCLUDING REMARKS

We have presented an electrostatic embedding QM/continuum model to compute the energetics and the spectroscopic properties of complex systems in heterogeneous environments. Our treatment is particularly intended for the study of proteins and membranes (as shown by the study of His140 pK_a in prion and of the tempo radical in DPPC) but it is not limited to these cases: it can be applied to any system partially embedded in environments with different polarity, provided a reliable estimate of the effective dielectric constants is available. It is much faster than QM-MM approaches based on different embedding techniques and does not suffer from any convergence problem. For instance, treatment of His140 in the heterogeneous PCM framework reduces the dimension of the electrostatic problem (i.e., the number of surface charge to be computed) from 71 164 (whole protein

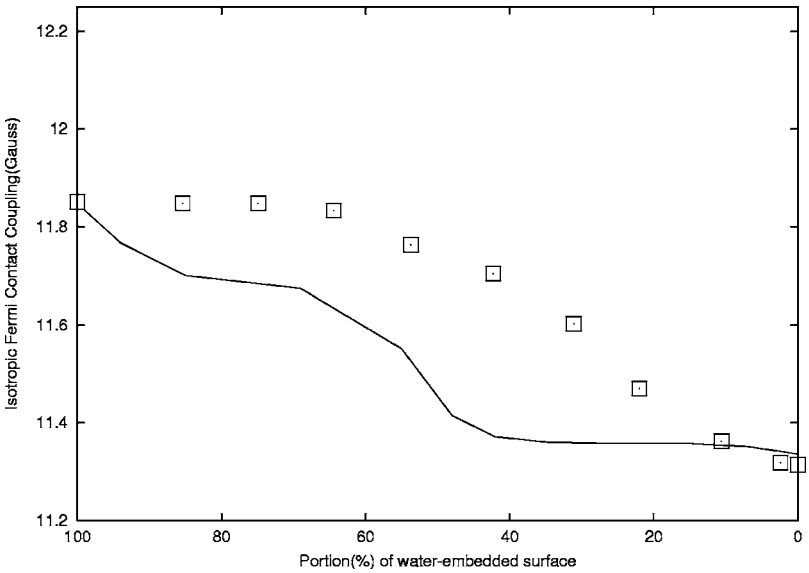

FIG. 6. The isotropic Fermi contact coupling (gauss) of Tempo across the membrane, with respect to the portion of water embedded surface. Points and solid line refer to the tempo approaching the membrane with the N–O bond perpendicular and along the z axis, respectively.

in water) to 759 (His140 embedded in the water/protein environment) solvation charges. On the other hand, our procedure should not be considered only as an alternative, but also a possible complement to other atomistic approaches. Just to make an example, snapshots of molecular dynamics (MD) simulations can be used to define the separation surface between the two media and to build the cavity to be used in a subsequent PCM calculations.

Furthermore, the implementation of the model in a general quantum-mechanical framework allows not only the computation of strutural and thermodynamic quantities, but also of different spectroscopic properties. For instance, the results obtained for the tempo radical embedded in a model membrane pave the route toward more reliable interpretations of spin probing experiments in terms of different placements of the probe on the macromolecular surface.

The main parameter required by the model is an effective dielectric constant, which can be determined, for instance, by comparison between the results obtained by the present procedure and those provided by conventional embedding techniques, and then used for further calculations in the same enviroment. As for the prion protein, we found quite a low value for the effective dielectric constant, though fully compatible with the values commonly used. However, our system was surface exposed, and thus the effect of the proteic environment should be smaller than for a residue in the interior of the protein. Furthermore, the only strong electrostatic interaction of His140, that with Asp147, was explicitly included in model II (and it would have been underestimated by a continuum model). Only taking into account a large number of representative systems would provide a reliable estimate of the "best average value" of the effective dielectric constant of a protein. This is obviously outside the scope of the present paper, that is aimed only to suggest a possible procedure to accomplish this task.

From another point of view, even if our approach has been developped in the framework of PCM, it can be easily extended to other solvation models. We think, however, that the physical soundness of PCM within both quantum-mechanical and classical frameworks gives more confidence on its reliability and range of applicability. Furthermore, although not yet widely recognized, recent developments led to a very effective linear scaling implementation, which is, at least, competitive with alternative models also for large systems. More generally, continuum models are the methods of choice in all cases where structural information at an atomistic level is not available or the increased computational cost is not warranted.

ACKNOWLEDGMENTS

The financial support of MIUR and INSTM are gratefully acknowledged. All the calculations have been performed at "Campus Computational Grid"-Università di Napoli "Federico II" advanced computing facilities.

[1] P. B. Karadakov and K. Morokuma, Chem. Phys. Lett. **317**, 589 (2000).
[2] G. A. Rickard, P. B. Karadakov, B. Peter, G. A. Webb, and K. Morokuma, J. Phys. Chem. A **107**, 292 (2003).
[3] M. Klaehn, J. Schlitter, and K. Gerwert, Biophys. J. **88**, 3829 (2005).
[4] S. Moon, S. Patchkovskii, and D. R. Salahub, THEOCHEM **632**, 287 (2003).
[5] F. Blomgren and S. Larsson, J. Phys. Chem. B **109**, 9104 (2005).
[6] A. Sinicropi, T. Andruniow, N. Ferre, R. Basosi, and M. Olivucci, J. Am. Chem. Soc. **127**, 11534 (2005).
[7] C. M. Bathelt, J. Zurek, A. J. Mulholland, and J. N. Harvey, J. Am. Chem. Soc. **127**, 12900 (2005).
[8] F. Graeter, S. M. Schwarzl, A. Dejaegere, S. Fischer, and J. C. Smith, J. Phys. Chem. B **109**, 10474 (2005).
[9] V. Barone, R. Improta, and N. Rega, Theor. Chem. Acc. **111**, 237 (2004).
[10] D. Riccardi, P. Schaefer, and Q. Cui, J. Phys. Chem. B **109**, 17715 (2005).
[11] J. H. Jensen, H. Li, A. D. Robertson, and P. A. Molina, J. Phys. Chem. A **109**, 6634 (2005).
[12] H. A. Stern and E. S. Feller, J. Chem. Phys. **118**, 3401 (2003).
[13] S. Tanizaki and M. Feig, J. Chem. Phys. **122**, 124706 (2005).
[14] W. Im, M. Feig, and C. L. Brooks III, Biophys. J. **85**, 2900 (2003).
[15] I. Oren, S. J. Fleishman, H. Kessel, and N. Ben-Tal, Biophys. J. **87**, 768 (2004).
[16] C. N. Schutz and A. Warshel, Proteins **44**, 400 (2001).
[17] S. Miertus, E. Scrocco, and J. Tomasi, Chem. Phys. **55**, 117 (1981).
[18] E. Langella, R. Improta, and V. Barone, Biophys. J. **87**, 3623 (2004).
[19] R. Improta, F. Mele, O. Crescenzi, C. Benzi, and V. Barone, J. Am. Chem. Soc. **124**, 7857 (2002).

[20] H. Li, C. S. Pomelli, and J. H. Jensen, Theor. Chem. Acc. **109**, 71 (2003).
[21] J. Tomasi and M. Persico, Chem. Rev. (Washington, D.C.) **94**, 2027 (1994).
[22] C. Benzi, M. Cossi, and V. Barone, J. Chem. Phys. **123**, 194909 (2005).
[23] C. Benzi, M. Cossi, V. Barone, R. Tarroni, and C. Zannoni, J. Phys. Chem. B **109**, 2584 (2005).
[24] H. Hoshi, M. Sakurai, Y. Inoue, and R. Chujo, J. Chem. Phys. **87**, 1107 (1987).
[25] L. Frediani, R. Cammi, S. Corni, and J. Tomasi, J. Chem. Phys. **120**, 3893 (2004).
[26] L. Frediani, C. S. Pomelli, and J. Tomasi, Phys. Chem. Chem. Phys. **2**, 4876 (2000).
[27] H. Li, A. W. Hains, J. E. Everts, A. D. Robertson, and J. H. Jensen, J. Phys. Chem. B **106**, 3486 (2002); Y. H. Jang, W. A. Goddard III, K. T. Noyes, L. C. Sowers, S. Hwang, and D. S. Chung, *ibid.* **107**, 344 (2003); H. W. van Vlijmen, M. Schaefer, and M. Karplus, Proteins **33**, 145 (1998); J. Kim, J. Mao, and M. R. Gunner, J. Mol. Biol. **348**, 1283 (2005); M. M. Naor and J. H. Jensen, Proteins **57**, 799 (2004).
[28] S. B. Prusiner, Science **252**, 1515 (1991).
[29] S. B. Prusiner, M. P. McKinley, K. A. Bowman, D. C. Bolton, P. E. Bendheim, D. F. Groth, and G. G. Glenner, Cell **35**, 349 (1983).
[30] W. Swietnicki, R. Petersen, P. Gambetti, and W. K. Surewicz, J. Biol. Chem. **272**, 27517 (1997).
[31] G. S. Jackson, A. F. Hill, C. Joseph, L. Hosszu, A. Power, J. P. Waltho, A. R. Clarke, and J. Collinge, Biochim. Biophys. Acta **1431**, 1 (1999).
[32] S. Hornemann and R. Glockshuber, Proc. Natl. Acad. Sci. U.S.A. **95**, 6010 (1999).
[33] D. O. V. Alonso, S. J. DeArmond, F. E. Cohen, and V. Daggett, Proc. Natl. Acad. Sci. U.S.A. **98**, 2985 (2001).
[34] D. O. V. Alonso, C. An, and V. Daggett, Philos. Trans. R. Soc. London, Ser. A **360**, 1165 (2002).
[35] E. Langella, R. Improta, and V. Barone, Biophys. J. **87**, 3623 (2004).
[36] *Spin Labeling: Theory and Applications*, edited by L. J. Berliner (Academic, New York, 1976).
[37] J. F. W. Keana, Chem. Rev. (Washington, D.C.) **78**, 37 (1978).
[38] B. R. Knauer and J. J. Napier, J. Am. Chem. Soc. **98**, 4395 (1976).
[39] R. N. Schwartz, M. Peric, S. A. Smith, and B. L. Bales, J. Phys. Chem. **101**, 8735 (1997).
[40] R. Improta and V. Barone, Chem. Rev. (Washington, D.C.) **104**, 1231 (2004).
[41] C. Amovilli, V. Barone, R. Cammi, E. Cances, M. Cossi, B. Mennucci, C. S. Pomelli, and J. Tomasi, Adv. Quantum Chem. **32**, 227 (1998).
[42] D. M. Chipman, J. Chem. Phys. **104**, 3276 (1996); **106**, 10194 (1997); C.-G. Zhan and D. M. Chipman, *ibid.* **110**, 1611 (1999); D. M. Chipman, *ibid.* **110**, 8012 (1999); **112**, 5558 (2000); Theor. Chem. Acc. **107**, 80 (2002).
[43] A. Klamt and V. Jonas, J. Chem. Phys. **103**, 9312 (1995).
[44] M. Cossi, N. Rega, G. Scalmani, and V. Barone, J. Chem. Phys. **114**, 5691 (2001).
[45] M. Cossi, N. Rega, G. Scalmani, and V. Barone, J. Chem. Phys. **117**, 43 (2002).
[46] A. Klamt and G. Schüürmann, J. Chem. Soc., Perkin Trans. 2 **1993**, 799; A. Klamt, *Cosmo-RS, from Quantum Chemistry to Fluid Phase Thermodynamics and Drugs Design* (Elsevier Science, New York, 2005); M. Hornig and A. Klamt, J. Chem. Inf. Model **45**, 1169 (2005).
[47] V. Barone and M. Cossi, J. Phys. Chem. A **102**, 1995 (1998).
[48] M. Cossi, N. Rega, G. Scalmani, and V. Barone, J. Comput. Chem. **24**, 669 (2003).
[49] V. Barone, M. Cossi, and J. Tomasi, J. Chem. Phys. **107**, 3210 (1997).
[50] J.-L. Pascual-Ahuir, E. Silla, and I. Tuñon, J. Comput. Chem. **15**, 1127 (1994).
[51] G. Scalmani, N. Rega, M. Cossi, and V. Barone, J. Comput. Methods Sci. Eng. **2**, 469 (2002).
[52] S. Tanizaki and M. Feig, J. Chem. Phys. **122**, 124706 (2005).
[53] H. A. Stern and S. E. Feller, J. Chem. Phys. **118**, 3401 (2003).
[54] M. J. Frisch *et al.*, computer code GAUSSIAN 03, Revision C.02 (Gaussian, Wallingford, CT, 2004).
[55] C. Adamo and V. Barone, J. Chem. Phys. **110**, 6158 (1999).
[56] C. Adamo, G. E. Scuseria, and V. Barone, J. Chem. Phys. **111**, 2889 (1999); C. Adamo and V. Barone, Chem. Phys. Lett. **314**, 152 (1999); C. Adamo and V. Barone, Theor. Chem. Acc. **105**, 169 (2000).
[57] L. Calzolai and R. Zahn, J. Biol. Chem. **278**, 35592 (2003).